American Journal of Preventive Cardiology 29 (2026) 101656

Contents lists available at ScienceDirect

American Journal of Preventive Cardiology

journal homepage: www.journals.elsevier.com/american-journal-of-preventive-cardiology

Comparing incidence of heart failure in individuals with enlarged cardiac chambers versus diabetes☆

Seyed Reza Mirjalili [a], Kyle Atlas [a], Anthony P. Reeves [b], Chenyu Zhang [a], Jakob Wasserthal [c], Amir Azimi [a], Ali Hashemi [a], Mohammadhossein Mozafarybazargany [a], Amir Ghaffari Jolfayi [a], Thomas Atlas [d], Claudia I. Henschke [e], David F. Yankelevitz [e], Javier J. Zulueta [e], Jeffrey Mechanick [f], Andrea D Branch [e], Ning Ma [e], Rowena Yip [e], Wenjun Fan [g], Sion K. Roy [h], Khurram Nasir [i], Sabee Molloi [j], Zahi Fayad [e], Michael V. McConnell [k], Ioannis A. Kakadiaris [l], George Abela [m], Rozemarijn Vliegenthart [n], David J. Maron [k], Jagat Narula [o], Kim A. Williams Sr [p], Prediman K. Shah [q], Matthew J. Budoff [h], Daniel Levy [r], Roxana Mehran [e], Robert A. Kloner [s,t], Nathan D. Wong [u], Morteza Naghavi [a,*]

[a] HeartLung.AI, Houston, TX 77021, USA
[b] Department of Electrical and Computer Engineering, Cornell University, Ithaca, NY 14853, USA
[c] University of Basel, Switzerland, Basel 4001, Switzerland
[d] Tustin Teleradiology, Tustin, CA 92780, USA
[e] Icahn School of Medicine at Mount Sinai, New York, NY 10029, USA
[f] Kravis Center for Clinical Cardiovascular Health, Mount Sinai Fuster Heart Hospital, New York, NY 10029, USA
[g] Department of Epidemiology and Biostatistics, Wen School of Public Health, University of California, Irvine, USA
[h] The Lundquist Institute, CA 90502, USA
[i] Houston Methodist Hospital, Houston, TX 77030, USA
[j] Department of Radiology, University of California Irvine, CA 92697, USA
[k] Stanford Prevention Research Center, Stanford University School of Medicine, Stanford, CA 94305, USA
[l] Computational Biomedicine Laboratory, Department of Computer Science, University of Houston, Houston, TX, USA
[m] Division of Cardiology, Michigan State University, East Lansing, MI 48823, USA
[n] Dept of Radiology, University Medical Center Groningen, GZ 9713, the Netherlands
[o] University of Houston, Houston, TX 77030, USA
[p] University of Louisville, Louisville, KY 40292, USA
[q] Cedars-Sinai Medical Center, Los Angeles, CA 90048, USA
[r] Population Sciences Branch, Division of Intramural Research, National Heart, Lung, and Blood Institute, National Institutes of Health, Bethesda, MD 20824, USA
[s] Huntington Medical Research Institutes, Pasadena, CA 91105, USA
[t] Keck School of Medicine of University of Southern California, Los Angeles, CA 90033, USA
[u] Heart Disease Prevention Program, Mary and Steve Wen Cardiovascular Division, University of California Irvine, CA 92697, USA

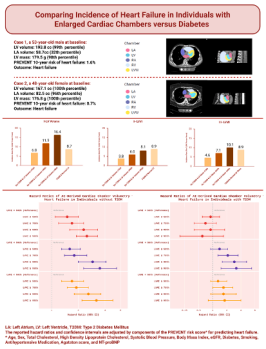
☆ An AI-CVD study within Pooled Cohort of Multi-Ethnic Study of Atherosclerosis and Framingham Heart study

* Corresponding author.
E-mail address: mn@vp.org (M. Naghavi).

https://doi.org/10.1016/j.ajpc.2026.101656

Available online 29 April 2026
2666-6677/© 2026 The Authors. Published by Elsevier B.V. This is an open access article under the CC BY-NC-ND license (http://creativecommons.org/licenses/by-nc-nd/4.0/).

GRAPHICAL ABSTRACT



ARTICLE INFO

Keywords:
Heart failure
Diabetes mellitus
Heart atria
Heart ventricle
Artificial intelligence
Diagnostic imaging

ABSTRACT

Background: Opportunistic cardiac chamber volumetry derived from coronary artery calcium (CAC) scans using the AI-CVD platform predicts heart failure (HF) independent of conventional risk factors. Type 2 diabetes mellitus (T2DM), which classifies individuals as Stage A HF, is associated with chamber enlargement; however, the HF risk associated with chamber enlargement in the absence of T2DM has not been characterized.

Methods: We analyzed left atrial (LA) and left ventricular (LV) volumes and mass, indexed to body surface area, using AI-CVD chamber volumetry of 7585 asymptomatic participants in the pooled cohort of Multi-Ethnic Study of Atherosclerosis (MESA) and Framingham Heart Study (FHS) second, and third generation (MESA & FHS; mean age 62.7 ± 14.6 years, 48.6 % male, 10.6 % with T2DM). Chambers were classified as enlarged (≥95th) or normal (<50th percentile). Cox regression and Kaplan–Meier analyses with log-rank tests were performed.

Results: Over a median follow-up of 17.1 years, 438 HF events occurred. Individuals without T2DM, with enlarged chambers had HF incidence rates comparable to or higher than individuals with T2DM and normal chambers: LA volume 16.4 vs 8.7 ($p = 0.001$), LV volume 8.1 vs 8.9 ($p = 0.66$), and LV mass 10.1 vs 8.9 ($p = 0.55$) per 1000 person-years. After multivariable adjustment, compared with normal chambers, enlarged LA (HR 2.5[1.9–3.3]), LV (HR 3.5[2.3–5.4]), and LV mass (HR 3.2[2.2–4.9]) remained independently associated with HF in individuals without T2DM.

Conclusion: AI-derived cardiac chamber enlargement measured in CAC scans is associated with HF incidence in individuals without T2DM, supporting its potential utility in HF risk stratification.

1. Introduction

Heart failure (HF) affects an estimated 64.3 million people worldwide, with a prevalence of about 2 % and an incidence ranging from 1 to 20 cases per 1000 person-years, posing a major global public health challenge [1]. Furthermore, it imposes a significant economic burden in the United States (US), with costs estimated to reach $70 billion by 2030 [2]. Given that HF can be asymptomatic in its early stages, screening and early detection are critical for improving outcomes and reducing healthcare costs [3].

Type 2 diabetes mellitus (T2DM) is a significant risk factor for HF, associated with a 2.4- to 5-fold increased risk [4]. Current US and European HF guidelines designate people with T2DM as Stage A (at risk) HF and recommend healthy lifestyle changes or even sodium-glucose cotransporter-2 (SGLT2) inhibitors for prevention of clinically overt HF [5]. However, relying solely on T2DM status and existing staging criteria overlooks substantial heterogeneity in risk [3,6]. Many individuals at high risk for HF fall outside the current staging framework, underscoring the need for more refined approaches to early identification [6].

A potentially promising approach for refining risk assessment is the evaluation of cardiac structure. Although this concepts is partially incorporated into existing HF guidelines, which classify left ventricular hypertrophy (LVH) as Stage B HF, current risk assessment primarily relies heavily on echocardiography and does not adequately consider the prognostic importance of left ventricular (LV) and left atrial (LA) volumes [3,5]. A large body of evidence links T2DM to various structural chamber alterations [4,7,8]; however, measurement of these structural alterations is not currently part of routine screening in asymptomatic individuals and is typically performed only in the context of specific clinical indications. Identifying enlarged cardiac chambers in addition to LVH may improve our ability to recognize individuals in the preclinical phases of HF, regardless of T2DM status.

In this context, chest CT imaging plays a crucial role. Chest imaging is one of the most frequently performed computed tomography (CT) examinations in the US, with approximately 15 million scans conducted annually presenting a valuable opportunity to evaluate the prognostic significance of cardiac structure [9,10]. Most chest CT images are non-contrast. Using traditional methods, it is difficult to distinguish the myocardium from blood and to identify valve planes required for accurate assessment of chamber size and myocardial mass in these scans [9]. However, recent advances in artificial intelligence (AI) enable reliable estimation of these metrics from non-contrast CT scans [11,12].

Prior research demonstrated that AI-derived chamber volumetry from non-contrast chest CT is a predictor of HF [13] and associated hospitalizations [14], atrial fibrillation [15,16], myocardial infarction [14], stroke [15], major cardiovascular events [17], and mortality [9]. However, none of these studies assessed the interaction between T2DM and chamber volumetry. Therefore, in this study we aimed to determine whether the AI-assessed chamber volumetry is associated with HF independent of T2DM status in a diverse asymptomatic population.

2. Methods

2.1. Study population

This analysis was conducted using pooled data from the Multi-Ethnic Study of Atherosclerosis (MESA)(https://mesa-nhlbi.org) and the Framingham Heart Study (FHS) second (Gen 2) and third generations (Gen 3) (https://www.framinghamheartstudy.org). MESA is a large, prospective, multicenter cohort study initiated between 2000 and 2002 at six U.S. field centers: Baltimore, MD; Los Angeles, CA; Chicago, IL; Forsyth County, NC; New York City, NY; and St. Paul, MN. The MESA cohort was comprised of individuals aged 45–84 without clinically apparent cardiovascular disease (CVD) at baseline. Initial assessments encompassed comprehensive medical histories, physical examinations, laboratory testing, and ECG-gated non-contrast CT scans for CAC scoring (80 % of RR-interval electron beam CT [EBCT] and 50 % of RR-interval for multidetector CT [MDCT]). Participants with a history of clinical CVD, physician-diagnosed angina, or prior invasive cardiovascular procedures, including coronary artery bypass grafting, percutaneous coronary intervention, valve replacement or repair, pacemaker implantation, or vascular surgery, were excluded. MESA recruited 6814 individuals, comprising men and women. However, 771 participants who did not consent to the use of their data by commercial entities, 151 cases with missing slices for the non-contrast CT scan, 9 with Type 1 diabetes, 59 patients with AI-CVD segmentation failure, 72 patients with atrial fibrillation and 22 individuals missing HF status after follow-up or time to event were excluded from our study (Fig. 1).

The FHS Gen 2 cohort was established in 1971, enrolling 5124 participants comprising biological children of the original Framingham cohort members and their spouses. The FHS Gen 3 cohort was initiated between 2002 and 2005, enrolling 4095 adult children (aged 19–72 years) of Gen 2 participants. Both cohorts were predominantly White. The present analysis utilized data from the FHS MDCT sub-study conducted between 2002 and 2005. Covariate data were obtained from examination cycle 7 for Gen 2 and examination cycle 1 for Gen 3, selected based on temporal proximity to the MDCT sub-study. Eligibility for the MDCT sub-study required men to be aged ≥35 years and women to be aged ≥40 years and non-pregnant, with a maximum weight of 160 kg. Recruitment preferentially enrolled individuals from larger Framingham families residing in the greater New England area. A total of 3535 participants (1418 from Gen 2 and 2117 from Gen 3) underwent ECG-gated non-contrast chest CT scans at 50 % of the RR-interval. Follow-up examinations were conducted at intervals of approximately four to eight years [18,19]. For the FHS cohort, we excluded 325 participants who did not consent to commercial use of their data, 281 participants with missing outcome or time-to-event data, 302 participants with missing weight or height (required for body surface area [BSA] calculation), and 772 participants with missing covariates, predominantly Agatston score (Fig. 1). Detailed information about these two cohorts' CT scan protocols is provided in **Supplementary Materials**.

This study was conducted in accordance with the ethical principles of the Declaration of Helsinki. The MESA study protocol received approval from the Institutional Review Boards at each participating site and the National Heart, Lung, and Blood Institute. All participants provided written informed consent upon enrollment. Ethical approval for the FHS was granted by the Institutional Review Board at Boston University Medical Campus. The present analysis was structured according to the Strengthening the Reporting of Observational Studies in Epidemiology (STROBE) guidelines.

2.2. Outcome definition

As part of the MESA protocol, participants were contacted via telephone every 9–12 months during follow-up and asked to report any new CVD diagnoses. Furthermore, ICD codes for hospital admissions were assessed by MESA reviewers. The reviewers classified patients with an official diagnosis of HF as having "probable" or "definite" HF, whereas those without such a diagnosis were categorized as "absent" HF. For a "definite" diagnosis of HF, supplementary criteria such as pulmonary congestion on chest X-ray, ventricular dilation, impaired LV systolic function, or LV diastolic dysfunction on echocardiography were required. For this analysis, we included both "probable" and "definite" HF events. Asymptomatic HF was not an endpoint in the MESA study; hence, patients without HF symptoms, such as shortness of breath or edema, could not be classified as having HF [20].

Within the FHS, incident HF events were identified through ongoing, systematic surveillance, including periodic participant health assessments, review of clinical interactions within the cohort, and examination of relevant inpatient and outpatient medical records. All suspected HF events were independently reviewed and adjudicated by a panel of three Framingham investigators. HF was diagnosed according to the Framingham criteria, which require either the presence of two major criteria or one major criterion in combination with two minor criteria.

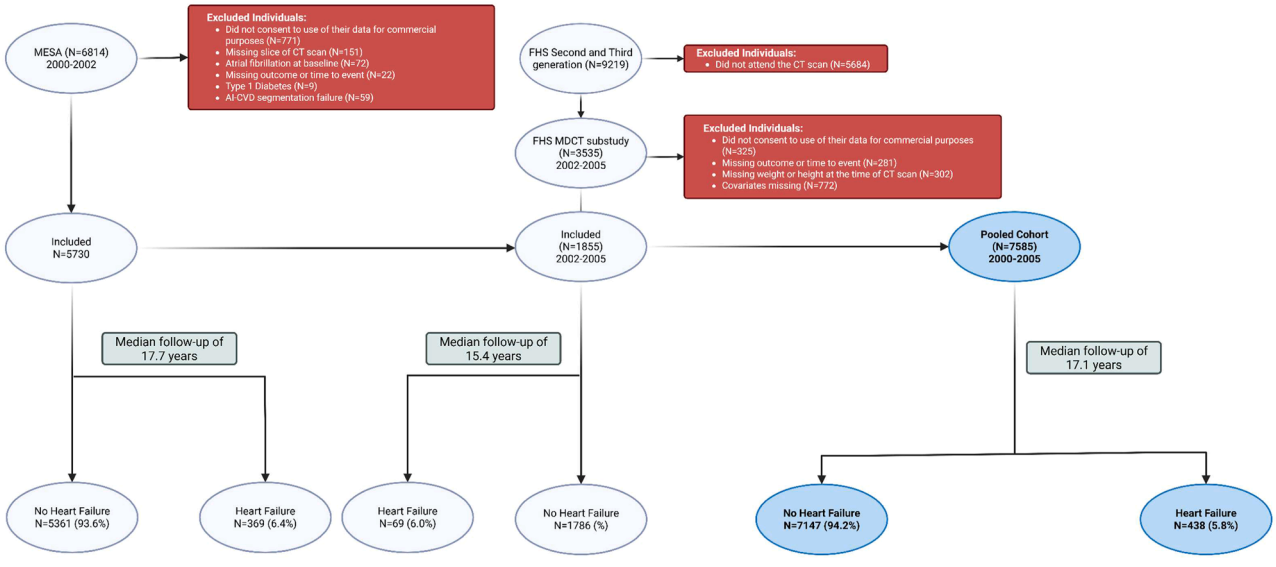


Fig. 1. Flow diagram of participant inclusion in the cohort.

Major diagnostic features included paroxysmal nocturnal dyspnea or orthopnea, elevated jugular venous pressure, pulmonary rales, radiographic evidence of cardiomegaly, acute pulmonary edema, a third heart sound, and hepatojugular reflux. Minor criteria encompassed peripheral edema, nocturnal cough, exertional dyspnea, hepatomegaly, radiographic pulmonary vascular congestion, pleural effusion, and a resting heart rate greater than 120 beats per minute. These findings were considered diagnostic only when they could not be explained by alternative clinical conditions. Additionally, a weight loss of at least 4.5 kg within five days following initiation of diuretic therapy was categorized as a major or minor criterion depending on the clinical circumstances [21]. Comparison of HF cumulative incidence between these two studies, are available in **Figure S1.**

2.3. AI-enabled chambers volumetry using non-contrast chest CT scans

We utilized a Food and Drug Administration (FDA) approved (K252029) AI-driven automated cardiac chamber volumetry tool, AutoChamber (HeartLung.AI, Houston, TX), which is integrated into the AI-CVD platform, to measure the volumes of the LA and LV as well as LV mass. AI-CVD is an AI-powered, multi-component system that analyzes non-contrast CT scans to identify hidden risks of diseases such as CVD, osteoporosis, and chronic obstructive pulmonary disease, enabling early intervention and personalized prevention strategies. Further details about AI-CVD and AutoChamber are available in the **Supplementary materials**.

2.4. Statistical analysis

All analyses were conducted using Python version 3.9.20. Continuous variables were presented with their mean ± standard deviation or median and interquartile range, while categorical variables were expressed as percentages. All tests of significance were two tailed, and significance was defined at the $p < 0.05$ level. Confidence intervals are presented at the 95 % level. To compare continuous variables between individuals with and without the outcome of HF, an independent samples *t*-test or Mann-Whitney U test was utilized, depending on the distribution of the variables. Chi-square tests were used to compare the frequency of categorical variables between those with and without HF according to T2DM status.

Given that chamber size strongly correlates with body size, we divided LA volume and LV volume and mass by BSA to compute the left atrial volume index (LAVI), left ventricular volume index (LVVI), and left ventricular mass index (LVMI) respectively. To explore potential non-linear associations between CT-derived cardiac chamber size measures and the risk of HF, we applied restricted cubic spline (RCS) modeling with three knots positioned at the 25th, 50th, and 75th percentiles of the exposure distribution. These spline functions were incorporated into age- and sex-adjusted Cox proportional hazards models, enabling assessment of hazard ratios (HR) across the continuous spectrum of chamber size values. Based on RCS analysis demonstrating HR approximating 1 for values below the 50th percentile with a linear increase thereafter, chamber sizes below the 50th percentile were selected as the reference category. Additional categories included ≥50th, ≥75th, ≥90th, and ≥95th percentiles. Comparisons between individuals without T2DM with enlarged chambers (≥50th, ≥75th, ≥90th, and ≥95th percentiles) and individuals with T2DM with normal chambers (<50th percentile) were performed using the Mid-P exact test for Poisson rates. As a supplementary analysis we applied the Benjamini-Hochberg false discovery rate (FDR) correction to these nine comparisons.

As a supplementary analysis, to quantify the population-level burden of HF attributable to chamber enlargement and T2DM, we calculated the population attributable risk (PAR), population attributable fraction (PAF) and relative risk (RR):

$$PAR = Incidence\ Rate\ in\ the\ Total\ population - Incidence\ Rate\ in\ Unexposed\ Individuals$$

$$PAF = \frac{PAR}{Incidence\ Rate\ in\ Total\ Population} \times 100$$

$$RR = \frac{Incidence\ Rate\ in\ Exposed\ Population}{Incidence\ Rate\ in\ Unexposed\ Population}$$

Bootstrap resampling (1000 iterations) was used to derive 95 % confidence intervals for PAR, PAF, and RR. Analyses were stratified by T2DM status to compare the population-level impact of chamber enlargement between individuals with and without T2DM.

Cox proportional hazards regression was used to evaluate the association between the previously mentioned categorizations of LAVI, LVVI and LVMI in both univariate and multivariate analyses. For all analyses, we employed measures below the 50th percentile as the reference group. The proportional hazards assumption was formally tested using Schoenfield residuals and found no significant violations. Covariates for multivariable analysis were selected based on the PREVENT risk score [22], a well-established tool for predicting HF and other CVD and also Agatston score and N-terminal pro-brain natriuretic peptide (NT-proBNP). Model 1 was adjusted for age, sex; Model 2 was adjusted for Model 1 plus smoking status, systolic blood pressure (SBP), total cholesterol, high density lipoprotein cholesterol (HDL-C), estimated glomerular filtration rate (eGFR), body mass index (BMI), and hypertension medication; Model 3 was adjusted for Model 2 plus logarithm of Agatston score; Model 4 was adjusted for Model 3 plus logarithm of NT-proBNP.

Kaplan-Meier analysis was utilized to examine the incidence ratios between individuals without T2DM with LAVI, LVVI, and LVMI exceeding the 95th percentile and patients with T2DM with normal chambers size (< 50th percentile), as well as those with both conditions. Group disparities were assessed utilizing the log-rank test. Similarly, as a supplementary analysis, the Benjamini–Hochberg FDR correction was applied to these nine comparisons.

3. Results

Study participants had a mean age of 62.7 ± 14.6 years at baseline; 48.6 % were male, and 10.6 % had T2DM. During 112,309 person-years of follow-up, with a mean duration of 14.8 ± 4.7 years, an HF incidence rate of 3.9 per 1000 person-years ($N = 438$) was observed. Table 1 presents the baseline characteristics of participants stratified by T2DM status and incident HF. Among individuals without T2DM, those who developed HF were older, more often male, and had higher BMI compared to those who did not develop HF. They also had higher creatinine, lower eGFR, higher glucose, and elevated NT-proBNP levels. Additionally, they demonstrated larger cardiac chamber volumes, higher systolic blood pressure, greater prevalence of hypertension, more frequent use of antihypertensive and lipid-lowering medications, and higher Agatston scores. Chinese ethnicity was less prevalent in this group.

Sex-specific cut points for chamber sizes (their BSA-indexed values) are provided in **Table S1**. The overall incidence ratio of HF for those without T2DM was 3.2 per 1000 person-years, and for patients with T2DM it was 11.2 per 1000 person-years ($P < 0.001$). Fig. 2 illustrates HF incidence rates per 1000 person-years according to chamber size percentiles, stratified by T2DM status. Among individuals without T2DM, HF incidence increased progressively with larger LAVI, rising from 1.6 in the <50th percentile to 16.4 per 1000 person-years in the ≥95th percentile (Fig. 2- a). Individuals with T2DM had higher incidence rates in each LAVI category; 8.7 per 1000 person-years in the <50th percentile and 29.0 in the ≥95th percentile. Similar patterns were observed for LVVI (Fig. 2- b) and LVMI (Fig. 2- c). For LVVI, incidence

Table 1
Baseline clinical characteristics participants according to type 2 diabetes status and incidence of heart failure.

	Without Type 2 Diabetes ($N = 6780$)			Type 2 Diabetes ($N = 805$)		
	No Heart failure ($N = 6457$)	Incident heart failure ($N = 323$)	P value	No Heart failure ($N = 690$)	Incident heart failure ($N = 115$)	P value
Age (years)	61.8 ± 14.6	72.8 ± 13.7	< 0.001	65.6 ± 12.0	70.4 ± 13.01	< 0.001
Sex (Male %)	47.6 %	56.0 %	0.004	52.5 %	60.9 %	0.1
Body mass index (kg/m²)	27.8 ± 5.2	29.4 ± 5.3	< 0.001	30.6 ± 6.0	31.01 ± 5.9	0.4
Race/Ethnicity						
White (%)	56.9 %	60.7 %	0.2	27.8 %	29.6 %	0.8
Chinese (%)	9.1 %	4.6 %	0.01	11.6 %	8.7 %	0.4
Black (%)	18.5 %	20.4 %	0.4	31.6 %	35.7 %	0.4
Hispanic (%)	15.5 %	14.2 %	0.6	29.0 %	26.1 %	0.6
Current smoker (%)	12.1 %	12.1 %	1	13.6 %	7.0 %	0.1
SBP (mmHg)	124.1 ± 19.8	134.5 ± 21.7	< 0.001	131.7 ± 20.8	138.4 ± 22.8	0.004
DBP (mmHg)	72.9 ± 10.0	72.8 ± 11.1	0.9	72.1 ± 10.5	72.6 ± 10.1	0.6
Hypertension (%)	44.0 %	67.0 %	< 0.001	66.8 %	80.9 %	0.004
Blood pressure medication consumption (%)	27.7 %	53.1 %	< 0.001	60.4 %	69.6 %	0.1
Total Cholesterol(mg/dl)	195.9 ± 35.1	191.9 ± 32.9	0.03	190.4 ± 40.0	185.6 ± 39.1	0.2
LDL-C (mg/dl)	118.4 ± 31.0	115.0 ± 29.8	0.05	112.7 ± 33.5	109.4 ± 35.7	0.4
HDL-C (mg/dl)	52.3 ± 15.5	50.4 ± 14.4	0.02	46.2 ± 13.2	45.3 ± 13.1	0.5
TG (Median, IQR) (mg/dl)	107.0 [75.0–156.0]	116.0 [78.2–161.0]	0.1	140.0 [91.0–204.0]	137.0 [102.5–195.0]	0.9
Dyslipidemia medication consumption (%)	14.0 %	19.8 %	0.004	27.8 %	29.6 %	0.8
Glucose (mg/dl)	91.2 ± 10.5	93.2 ± 11.4	0.001	152.8 ± 55.0	154.6 ± 62.1	0.8
Creatinine(mg/dl)	0.9 ± 0.2	1.0 ± 0.2	< 0.001	0.95 ± 0.50	1.10 ± 0.85	0.1
eGFR (mL/min)	81.4 ± 17.3	71.3 ± 16.5	< 0.001	81.0 ± 20.0	73.5 ± 21.7	< 0.001
Agatston CAC Score (Median, IQR)	0.0 [0.0–54.9]	108.4 [0.0–450.3]	< 0.001	22.3 [0.0–193.7]	126.2 [3.3–697.6]	< 0.001
NT-proBNP (Median, IQR) (pg/ml)	44.22 [19.7–89.9]	84.7 [39.0–188.5]	< 0.001	39.6 [18.1–98.0]	67.5 [20.9–135.4]	< 0.001
AI-derived Chambers Volumetry						
LAVI volume (mL)	30.0 ± 8.1	36.4 ± 10.5	< 0.001	30.3 ± 8.3	33.0 ± 9.8	0.01
LVVI wall mass (mL)	54.6 ± 11.4	58.5 ± 16.4	< 0.001	54.1 ± 11.7	59.3 ± 15.7	< 0.001
LVMI volume (g/m²)	53.7 ± 10.0	58.2 ± 15.0	< 0.001	54.1 ± 10.6	58.7 ± 14.1	0.001
PREVENT-HF predicted risk	0.04 [0.01–0.1]	0.12 [0.06–0.2]	< 0.001	0.13 [0.1–0.2]	0.2 [0.1–0.3]	< 0.001

LDL-C: Low density lipoprotein cholesterol, HDL-C: High density lipoprotein cholesterol, TG: Triglyceride, IQR: Interquartile ranges, NT-proBNP: N Terminal Brain natriuretic peptide, CAC: Coronary calcium scan, LVVI: Left ventricular volume index, LAVI: Left atrial volume index, LVMI: Left ventricular mass index, T2DM: Type 2 diabetes mellitus, SBP: Systolic blood pressure, DBP: Diastolic Blood pressure, eGFR: Estimated glomerular filtration rate, PREVENT-HF: Predicting Risk of Cardiovascular Disease EVENTs- Heart Failure equation.

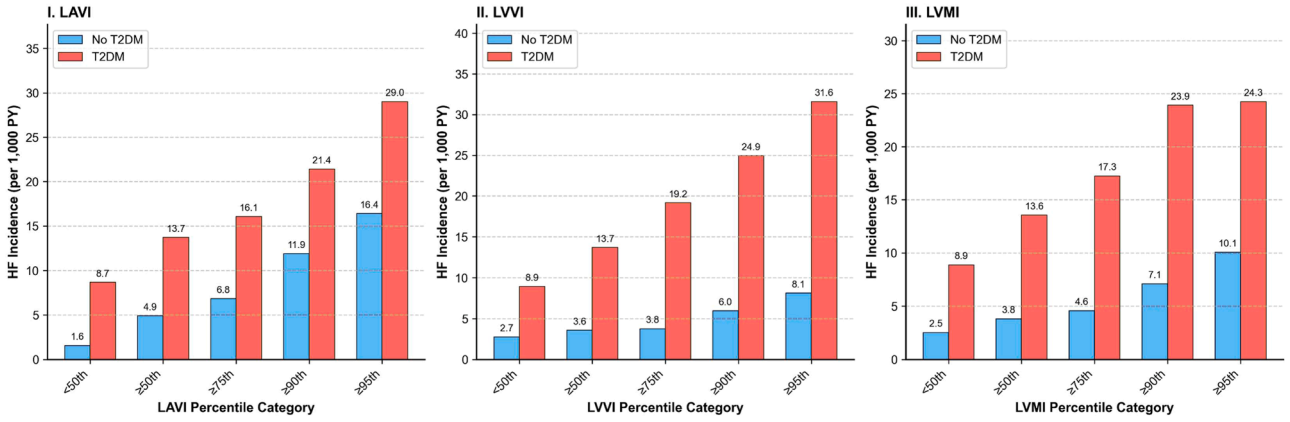


Fig. 2. Incidence of heart failure based on ai-derived left heart chamber sizes, stratified by type 2 diabetes mellitus status.
T2DM: Type 2 diabetes mellitus, LAVI: Left atrial volume index (LA volume / body surface area), LVVI: Left ventricular volume index (LV volume / body surface area), LVMI: Left ventricular myocardial index (LV mass / body surface area), AI: Artificial intelligence.

rates in individuals without T2DM rose from 2.7 to 8.1 per 1000 person-years from <50th to ≥95th percentile, while individuals with T2DM showed rates of 8.9 to 31.6 per 1000 person-years. For LVMI, individuals without T2DM had incidence rates increasing from 2.5 to 10.1 per 1000 person-years, compared with 8.9 to 24.3 per 1000 person-years in those with T2DM.

Fig. 3a–c compare HF incidence rates between individuals without T2DM with enlarged chambers and individuals with T2DM with normal chamber sizes (<50th percentile). For LAVI (Fig. 3a), individuals without T2DM with values ≥75th, ≥90th, and ≥95th percentile demonstrated incidence rates of 6.8, 11.9, and 16.4 per 1000 person-years, respectively, compared with 8.7 per 1000 person-years in individuals with T2DM with normal LAVI (p value = 0.16, p value = 0.07, and p value = 0.001, respectively). Notably, individuals without T2DM with LAVI ≥95th percentile had nearly double the HF incidence of individuals with T2DM with normal chambers. For LVVI (Fig. 3b), individuals without T2DM with values ≥75th, ≥90th, and ≥95th percentile had incidence rates of 3.8, 6.0, and 8.1 per 1000 person-years, compared with 8.9 per 1000 person-years in individuals with T2DM with normal LVVI (p value <0.001, p value = 0.04, and p value =0.66, respectively). For LVMI (Fig. 3c), incidence rates in individuals without T2DM at ≥75th, ≥90th, and ≥95th percentile were 4.6, 7.1, and 10.1 per 1000 person-years, compared with 8.9 per 1000 person-years in individuals with T2DM with normal LVMI (p value < 0.001, p value =0.24, and p value =0.55, respectively). All significant associations remained significant after Benjamini-Hochberg FDR correction for multiple comparisons (**Table S2**).

Fig. 4 displays cumulative incidence curves comparing HF risk among individuals without T2DM with chamber enlargement (≥95th percentile), individuals with T2DM with normal chambers (<50th percentile), and those with both conditions. For LAVI (Fig. 4a) individuals without T2DM with enlarged LAVI had significantly higher HF incidence compared to individuals with T2DM with normal LAVI. Those with both conditions had the highest cumulative incidence, significantly exceeding T2DM alone (LAVI < 50th percentile) (p value <0.001), while showing no significant difference compared to enlarged LAVI alone (p value =0.08). For LVVI (Fig. 4b), individuals without T2DM with enlarged LVVI demonstrated comparable HF incidence to individuals with T2DM with normal LVVI. However, those with both conditions had significantly higher incidence than either condition alone (both p value <0.001). For LVMI (Fig. 4c), individuals without T2DM with increased LVMI showed similar HF incidence to individuals with T2DM with normal LVMI. Combined T2DM and elevated LVMI conferred the highest risk, significantly exceeding both T2DM alone (p value <0.001) and elevated LVMI alone (p value = 0.01). All significant associations remained significant after Benjamini-Hochberg FDR correction for multiple comparisons (**Table S3**).

Restricted cubic spline analysis, adjusted for age and sex, revealed a continuous dose-response relationship between chamber size and HF risk (**Figure S2**). HRs increased monotonically across the distribution of LAVI, LVVI, and LVMI, with values below the 50th percentile demonstrating HR ~1.

PAF analysis demonstrated that LAVI ≥90th percentile accounted for 21.2 % (95 % CI: 16.6–25.8 %) of HF cases in the total population, exceeding the contribution of T2DM (18.8 %; 95 % CI: 14.6–23.5 %). LVMI and LVVI at the same threshold contributed to 12.5 % (95 % CI: 8.2–16.3 %) and 9.7 % (95 % CI: 5.8–13.5 %) of HF cases, respectively. Given that approximately 90 % of the population does not have T2DM, the majority of the population-level burden of HF attributable to chamber enlargement occurs among individuals without T2DM. This is particularly evident for LAVI, where the PAF was 25.3 % in individuals without T2DM compared to 9.2 % in those with T2DM (**Table S4**).

Table 2 presents the association between chamber size categories and HF risk stratified by T2DM status. In individuals without T2DM, enlarged LAVI, LVVI, and LVMI were significantly associated with higher HF risk across all percentile thresholds and adjustment models. In the crude model, individuals without T2DM with LAVI ≥95th percentile had a HR of 3.3 (95 % CI: 2.5–4.3). This association remained significant after sequential adjustment for age and sex (Model 1: HR 2.9; 95 % CI: 2.3–3.8), Model 1 plus PREVENT risk score components (Model 2: HR 2.7; 95 % CI: 2.1–3.5), Model 2 plus Agatston score (Model 3: HR 2.6; 95 % CI: 2.0–3.4), and Model 3 plus NT-proBNP (Model 4: HR 2.5; 95 % CI: 1.9–3.3). Similar patterns were observed for LVVI ≥95th percentile (Model 4 HR 3.5; 95 % CI: 2.3–5.4) and LVMI ≥95th percentile (Model 4 HR 3.2; 95 % CI: 2.2–4.9). Continuous analysis confirmed these findings, with HRs per 1-SD increase in the fully adjusted model (Model 4) of 1.2 (95 % CI: 1.1–1.3) for LAVI, 1.5 (95 % CI: 1.3–1.6) for LVVI, and 1.5 (95 % CI: 1.3–1.6) for LVMI.

Among individuals with T2DM, the association between chamber enlargement and HF risk varied by measure and level of adjustment. In Model 3, LVVI ≥95th percentile (HR 5.9; 95 % CI: 3.1–11.4) and LVMI ≥95th percentile (HR 3.3; 95 % CI: 1.7–6.5) were significantly associated with HF, whereas LAVI ≥95th percentile was not (HR 1.6; 95 % CI: 0.7–3.6). After additional adjustment for NT-proBNP (Model 4), LVVI ≥95th percentile remained significantly associated with HF (HR 3.2; 95 % CI: 1.5–6.5), while associations for LVMI (HR 1.8; 95 % CI: 0.8–4.0) was attenuated to non-significance. Continuous analysis demonstrated similar patterns, with HRs per 1-SD increase of 1.3 (95 % CI: 1.1–1.7) for LVVI remaining significant in the fully adjusted model. Supplementary analyses further demonstrated that individuals with prediabetes and enlarged cardiac chambers exhibited HF incidence rates and HRs intermediate between normoglycemic individuals and those with T2DM (**Figure S3–4** and **Table S5**), suggesting that the prognostic value of AI-derived chamber volumetry extends across the glycemic spectrum.

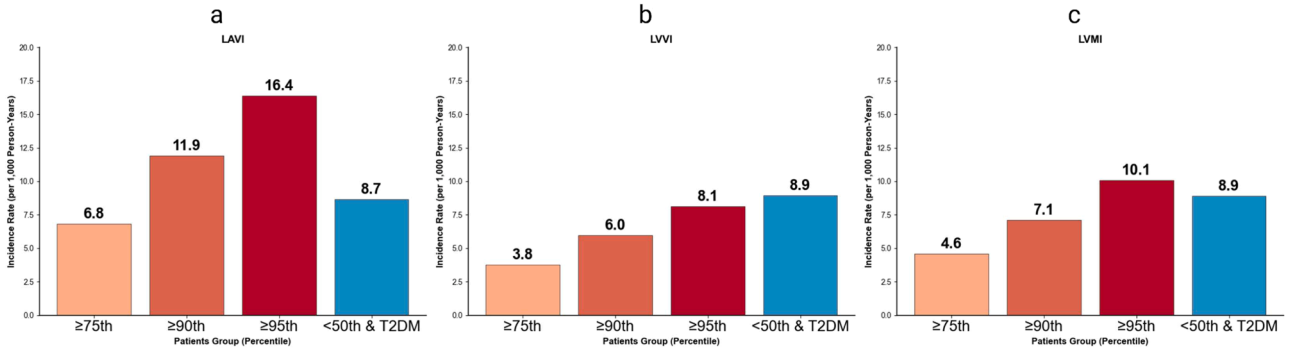


Fig. 3. Comparison of heart failure incidence between individuals with enlarged cardiac chambers without type 2 diabetes and those with type 2 diabetes without chamber enlargement.

T2DM: Type 2 diabetes mellitus, LAVI: Left atrial volume index (LA volume / body surface area), LVVI: Left ventricular volume index (LV volume / body surface area), LVMI: Left ventricular myocardial index (LV mass / body surface area).

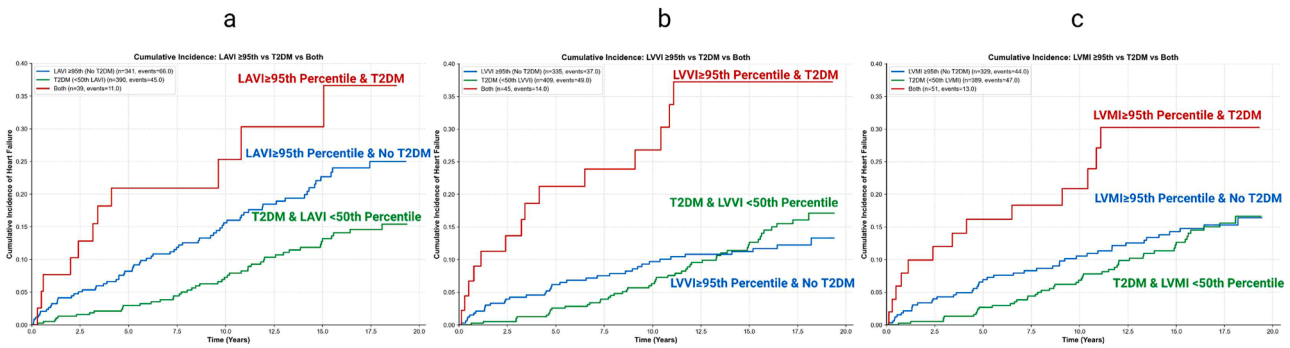


Fig. 4. Kaplan–Meier curves comparing heart failure incidence in participants with both type 2 diabetes and enlarged cardiac chambers versus either condition alone.

T2DM: Type 2 diabetes mellitus, LAVI: Left atrial volume index (LA volume / body surface area), LVVI: Left ventricular volume index (LV volume / body surface area), LVMI: Left ventricular myocardial index (LV mass / body surface area.

4. Discussion

This study demonstrates that AI-derived LA volume, LV volume, and LV mass from non-contrast CT scans are significantly associated with incident HF, including among individuals without T2DM. These findings support a potential role for opportunistic chamber volumetry in HF risk evaluation. Notably, individuals without T2DM with enlarged chambers (≥95th percentile) exhibited HF incidence rates comparable to or exceeding those of individuals with T2DM with normal chamber sizes, despite T2DM being an established Stage A HF equivalent. Furthermore, these associations remained significant after adjustment for clinically relevant risk factors, Agatston score, and NT-proBNP, suggesting that chamber volumetry captures risk information not fully reflected by established clinical and biochemical markers.

Numerous studies have reported a high prevalence of asymptomatic structural cardiac abnormalities such as increased LA and LV volume and increased LV mass in patients with T2DM [4,5,8]. However, these structural abnormalities are not specific to T2DM and can also be observed in euglycemic patients or patients with other risk factors such as hypertensive heart disease, coronary heart disease, aortic and mitral valve disorders, obesity, and chronic kidney disease, making cardiac chamber remodeling a more encompassing marker of HF risk than T2DM alone [23]. Our findings align with these observations, demonstrating that individuals with chamber enlargement, even in the absence of T2DM, exhibit HF incidence rates comparable to or exceeding those of individuals with T2DM with normal chamber sizes. Furthermore, the significant association between chamber volumetry and incident HF in individuals without T2DM reinforces the notion that structural remodeling identifies HF risk regardless of T2DM status.

Current clinical guidelines acknowledge the heightened risk of HF among individuals with T2DM [5,24]. The American Diabetes Association (ADA) recommends annual HF screening with NT-proBNP in this population [25]. In our study, however, cardiac chamber enlargement, particularly increased LV volume and mass, remained independently associated with incident HF even after adjustment for NT-proBNP, in both individuals with and without T2DM. Notably, the persistence of these associations in participants without T2DM, who are not routinely targeted for annual HF screening under current ADA recommendations, suggests that AI-derived chamber volumetry captures prognostic information beyond that provided by NT-proBNP alone.

In parallel, the American Heart Association (AHA) recommends echocardiographic evaluation and NT-proBNP measurement for individuals at borderline to high risk of HF as defined by the PREVENT-HF equation [26]. Our results extend these recommendations by demonstrating that AI-based chamber volumetric measures are associated with incident HF independently of both NT-proBNP and PREVENT-HF risk components. Together, these findings indicate that AI-derived chamber volumetry may offer complementary and incremental prognostic value beyond existing guideline-endorsed risk stratification approaches.

Beyond PREVENT-HF components and NT-proBNP, AI-derived chamber volumetry demonstrated a significant association with incident HF independent of the Agatston score. The Agatston score is the most commonly used metric derived from CAC scans and is primarily applied for coronary artery disease risk stratification; prior studies have also identified CAC as an independent predictor of HF [27–31]. The persistence of significant associations after adjustment for CAC suggests that AI-derived chamber volumetry captures complementary pathophysiological information beyond coronary atherosclerotic burden. This finding may be particularly important in non–T2DM populations, as current guidelines recommend statin therapy for adults with T2DM aged ≥40 years regardless of CAC score and most of the times do not support routine CAC testing for risk stratification in this group. Together, these results suggest that AI-derived chamber volumetry can expand the clinical utility of CAC scans beyond traditional CAC scoring.

Early identification of individuals at risk for HF, particularly during the preclinical stage, provides an important opportunity to intervene through lifestyle modification or established pharmacologic therapies [32]. Assessment of cardiac chamber size plays a key role in this process and can be performed using several imaging modalities, including echocardiography, CT, and cardiac magnetic resonance (CMR) [33–36]. Echocardiography is the most commonly used modality; however, it is operator-dependent, relies on adequate acoustic windows, and may have limitations in accurately delineating endocardial borders or visualizing all chamber components, particularly the atrial appendage [37]. CMR offers superior image quality and reproducibility but is constrained by limited availability, higher costs, and longer acquisition times, which restrict its use in large-scale or routine screening [38]. Although CT cannot replace echocardiography or CMR for detailed functional assessment, it offers several practical advantages for risk stratification, particularly as a screening rather than a diagnostic tool. Non-contrast CT scans are widely available, rapidly acquired, and less operator-independent, with relatively low cost and modest radiation exposure. Importantly, CT imaging is frequently performed for a variety of clinical indications beyond cardiovascular evaluation, enabling opportunistic assessment of cardiac chamber size without additional imaging or patient burden.

4.1. *Clinical implications and future directions*

Results of this study suggest potential clinical utility for opportunistic HF risk assessment; however, several questions remain before implementation in routine practice. First, although marked LA or LV enlargement may be qualitatively recognized by experienced readers on CAC scans and can occasionally prompt further clinical evaluation, routine CAC scan interpretation does not include standardized, quantitative assessment of cardiac chamber size or LV mass. As a result, these

Table 2
Heart failure risk based on AI-measured left heart chamber size stratified by T2DM status.

	Without T2DM				
	Crude model	Model 1	Model 2	Model 3	Model 4
Variable (Number/Events)	**HR (95 % CI)**	**HR (95 % CI)**	**HR (95 % CI)**	**HR (95 % CI)**	**HR (95 % CI)**
Categorical					
LAVI < 50th (3402/83)	1.0	1.0	1.0	1.0	1.0
LAVI ≥ 50th (3378/240)	3.2 (2.5–4.1)	2.2 (1.7–2.8)	2.0 (1.6–2.7)	2.0 (1.5–2.6)	1.5 (1.1–2.0)
LAVI ≥ 75th (1680/159)	4.5 (3.4–5.8)	2.8 (2.1–3.8)	2.6 (1.9–3.5)	2.5 (1.9–3.4)	1.7 (1.2–2.3)
LAVI ≥ 90th (668/102)	7.9 (5.9–10.5)	4.6 (3.3–6.3)	4.2 (3.0–5.9)	4.0 (2.8–5.6)	2.3 (1.6–3.3)
LAVI ≥ 95th (341/66)	3.3 (2.5–4.3)	2.9 (2.3–3.8)	2.7 (2.1–3.5)	2.6 (2.0–3.4)	2.5 (1.9–3.3)
LVVI < 50th (3383/140)	1.0	1.0	1.0	1.0	1.0
LVVI ≥ 50th (3397/183)	1.3 (1.0–1.6)	1.7 (1.3–2.1)	1.6 (1.3–2.0)	1.6 (1.3–2.0)	1.6 (1.3–2.1)
LVVI ≥ 75th (1704/95)	1.4 (1.0–1.8)	1.9 (1.4–2.4)	1.8 (1.4–2.4)	1.9 (1.4–2.5)	1.8 (1.4–2.5)
LVVI ≥ 90th (678/58)	2.2 (1.6–2.9)	3.1 (2.3–4.2)	2.9 (2.0–4.0)	3.0 (2.2–4.2)	2.9 (2.0–4.1)
LVVI ≥ 95th (335/37)	3.0 (2.1–4.3)	4.3 (3.0–6.2)	4.3 (2.9–6.4)	4.3 (2.9–6.4)	3.5 (2.3–5.4)
LVMI < 50th (3403/131)	1.0	1.0	1.0	1.0	1.0
LVMI ≥ 50th (3377/192)	1.5 (1.2–1.9)	1.8 (1.4–2.2)	1.7 (1.3–2.1)	1.7 (1.3–2.1)	1.7 (1.3–2.3)
LVMI ≥ 75th (1678/112)	1.8 (1.4–2.3)	2.3 (1.7–2.9)	2.0 (1.5–2.6)	2.0 (1.5–2.6)	1.9 (1.5–2.6)
LVMI ≥ 90th (666/66)	2.8 (2.1–3.8)	3.6 (2.7–4.9)	3.1 (2.2–4.2)	3.1 (2.2–4.2)	2.6 (1.8–3.6)
LVMI ≥ 95th (329/44)	4.0 (2.9–5.7)	5.0 (3.5–7.1)	4.1 (2.8–6.0)	4.0 (2.8–5.9)	3.2 (2.2–4.9)
Continuous					
LAVI per 1 SD	1.6 (1.5–1.6)	1.5 (1.4–1.6)	1.4 (1.3–1.5)	1.4 (1.3–1.5)	1.2 (1.1–1.4)
LVVI per 1 SD	1.3 (1.2–1.5)	1.5 (1.4–1.6)	1.5 (1.3–1.6)	1.5 (1.4–1.7)	1.5 (1.3–1.6)
LVMI per 1 SD	1.4 (1.3–1.6)	1.6 (1.5–1.7)	1.5 (1.4–1.7)	1.6 (1.4–1.7)	1.5 (1.3–1.7)
	With T2DM				
	Crude model	**Model 1**	**Model 2**	**Model 3**	**Model 4**
	HR (95 % CI)	**HR (95 % CI)**	**HR (95 % CI)**	**HR (95 % CI)**	**HR (95 % CI)**
LAVI < 50th (390/45)	1.0	1.0	1.0	1.0	1.0
LAVI ≥ 50th (415/70)	1.6 (1.1–2.3)	1.3 (0.9–2.0)	1.2 (0.8–1.8)	1.2 (0.8–1.7)	0.9 (0.6–1.4)
LAVI ≥ 75th (217/39)	1.9 (1.2–2.9)	1.4 (0.9–2.2)	1.3 (0.8–2.0)	1.2 (0.7–1.9)	0.7 (0.4–1.2)
LAVI ≥ 90th (91/20)	2.5 (1.5–4.3)	1.8 (1.0–3.1)	1.7 (0.9–3.0)	1.6 (0.9–2.9)	0.9 (0.4–1.8)
LAVI ≥ 95th (39/11)	3.4 (1.8–6.7)	2.5 (1.2–4.9)	1.9 (0.9–4.1)	1.6 (0.7–3.6)	0.6 (0.2–1.7)
LVVI < 50th (409/49)	1.0	1.0	1.0	1.0	1.0
LVVI ≥ 50th (396/66)	1.5 (1.1–2.2)	1.7 (1.2–2.5)	1.7 (1.2–2.5)	1.7 (1.1–2.5)	1.4 (0.9–2.1)
LVVI ≥ 75th (193/43)	2.1 (1.4–3.2)	2.8 (1.8–4.3)	3.0 (1.9–4.7)	2.9 (1.8–4.5)	2.1 (1.3–3.5)
LVVI ≥ 90th (81/22)	2.9 (1.7–4.8)	3.7 (2.2–6.2)	4.1 (2.4–7.2)	3.9 (2.2–7.0)	2.9 (1.6–5.3)
LVVI ≥ 95th (45/14)	3.6 (2.0–6.6)	4.3 (2.3–7.8)	5.6 (2.9–10.7)	5.9 (3.1–11.4)	3.2 (1.5–6.8)
LVMI < 50th (389/47)	1.0	1.0	1.0	1.0	1.0
LVMI ≥ 50th (416/68)	1.5 (1.1–2.2)	1.7 (1.2–2.5)	1.7 (1.1–2.5)	1.7 (1.1–2.5)	1.3 (0.9–2.0)
LVMI ≥ 75th (219/44)	1.9 (1.3–2.9)	2.3 (1.5–3.4)	2.3 (1.4–3.5)	2.2 (1.4–3.5)	1.7 (1.0–2.7)
LVMI ≥ 90th (93/24)	2.7 (1.7–4.5)	2.9 (1.8–4.8)	3.0 (1.8–5.2)	2.9 (1.6–5.1)	1.7 (0.9–3.2)
LVMI ≥ 95th (51/13)	2.8 (1.5–5.2)	3.0 (1.6–5.6)	3.4 (1.8–6.5)	3.3 (1.7–6.5)	1.8 (0.8–4.0)
Continuous					
LAVI per 1 SD	1.4 (1.2–1.7)	1.3 (1.1–1.5)	1.2 (1.0–1.5)	1.2 (1.0–1.45)	0.9 (0.7–1.1)
LVVI per 1 SD	1.5 (1.3–1.8)	1.6 (1.3–1.8)	1.6 (1.3–1.9)	1.7 (1.4–2.0)	1.3 (1.1–1.7)
LVMI per 1 SD	1.5 (1.3–1.8)	1.5 (1.3–1.8)	1.5 (1.3–1.8)	1.6 (1.3–1.9)	1.3 (1.03–1.6)

Model 1: Adjusted for age, sex.
Model 2: Model 1+ smoking, systolic blood pressure, total cholesterol, high density lipoprotein cholesterol, creatinine, body mass index, hypertension medication (PREVENT predicting risk score components).
Model 3: Model 2 + Agatston score.
Model 4: Model 3 + NT-proBNP.
T2DM: Type 2 diabetes mellitus, AI: Artificial intelligence, LAVI: left atrial volume index, LVVI: Left ventricular volume index, SD: Standard deviation, HR: Hazard ratio.

structural findings are not systematically reported. Moreover, current clinical guidelines do not define CT-based thresholds for chamber enlargement or hypertrophy in the setting of non-contrast CT imaging. Consequently, structural cardiac remodeling is often under-recognized and inconsistently addressed in routine practice. These gaps highlight the need for future studies to establish normative reference values for cardiac chamber size using ECG-gated non-contrast CT scans. Second, future studies should evaluate whether incorporating AI-derived chamber volumetry into existing HF risk prediction algorithms, such as PREVENT-HF, improves discriminative performance and risk reclassification. Third, clinical trials are needed to determine whether early intervention in asymptomatic individuals with chamber enlargement can effectively prevent or delay progression to symptomatic HF, and whether such strategies are cost-effective. Fourth, the generalizability of our findings to non-gated CT acquisitions warrants investigation, as non-gated scans are more commonly performed in clinical practice and would substantially expand the potential population for opportunistic screening. Addressing these questions will be essential for translating the observed associations into meaningful improvements in HF prevention and early detection strategies.

4.2. Limitations

The present study has several limitations. MESA baseline CT scans were conducted from 2000 to 2002 employing electron-beam computed tomography (EBCT) or previous models of multidetector CT (MDCT) scanners, but contemporary CAC scanning employs more sophisticated MDCT technology. Nevertheless, as our AI training was conducted entirely outside of MESA and utilized a modern MDCT (256 slices) scanner, we do not think this impacts on the generalizability of our results. Although the mean follow-up of 14.8 ± 5.2 years provides insight into the lifetime risk of HF, we used only a single baseline measurement

of LA and LV volume and LV mass and T2DM status and did not capture changes in these metrics over time. While these factors may change over time before the onset of HF, assuming such changes occur randomly, they are unlikely to significantly impact on our findings. MESA only investigated symptomatic individuals to define HF outcome, increasing the risk of underdiagnosis by missing asymptomatic patients. We were unable to perform subtype-specific analyses for HF with preserved ejection fraction (HFpEF) and HF with reduced ejection fraction (HFrEF). Although MESA includes data on HF subtype classification, a substantial proportion of incident HF cases were not categorized by ejection fraction and remain classified as unknown subtype. Excluding these cases would introduce selection bias and reduce statistical power. Furthermore, FHS does not provide HF subtype classification, precluding harmonized subtype-specific analyses across cohorts. Given that the association between chamber enlargement and HF may differ by subtype, particularly across T2DM where HFpEF is more prevalent, future studies with comprehensive ejection fraction data are needed to evaluate whether AI-derived chamber volumetry differentially associates with HFpEF versus HFrEF in populations with and without T2DM. Additionally, HbA1c levels and duration of T2DM diagnosis were not available, precluding adjustment for glycemic control or diabetes duration. A further drawback is the potential influence of varying ECG gating techniques (RR-interval) employed in MESA for multidetector (MD)CT (50 %) and Electron beam (EB)CT (80 %). This variation resulted in notable differences in LA volume measurements, with smaller values obtained using EBCT compared with MDCT (57.4 mL vs. 65.4 mL; $p < 0.0001$). By contrast, LV volume measurements were comparable across scanner types (**Table S6**). Although we adjusted for multiple cardiovascular risk factors, residual confounding from unmeasured variables. Finally, our analysis removed 771 cases that did not provide consent for use of their data by commercial entities. Nevertheless, the baseline features of these cases did not exhibit systematic differences compared with the other participants.

5. Conclusion

Our findings suggest that opportunistic, AI-enabled identification of LA and LV enlargement, as well as increased LV mass, from CAC scans is independently associated with incident HF, regardless of T2DM status. This approach may facilitate the identification of individuals without T2DM who remain at elevated risk for HF and could benefit from earlier preventive interventions. Moreover, participants with both T2DM and structural cardiac enlargement exhibited the highest rates of HF incidence, indicating a subgroup that may warrant more intensive preventive strategies. By enabling assessment of structural cardiac remodeling in addition to coronary calcium burden, AI-driven cardiac chamber volumetry expands the clinical utility of CAC scans beyond traditional risk stratification and represents a promising strategy for earlier identification of individuals at increased risk for heart failure, meriting further investigation.

List of abbreviations

ADA: American Diabetes Association
AHA: American Heart Association
AI: Artificial Intelligence
BMI: Body Mass Index
BSA: Body Surface Area
CAC: Coronary Artery Calcium
CI: Confidence Interval
CMR: Cardiac Magnetic Resonance
CT: Computed Tomography
CVD: Cardiovascular Disease
EBCT: Electron-Beam Computed Tomography
ECG: Electrocardiogram eGFR: Estimated Glomerular Filtration Rate
FDA: Food and Drug Administration
FDR: False Discovery Rate
FHS: Framingham Heart Study
Gen 2: Second Generation
Gen 3: Third Generation
HDL-C: High-Density Lipoprotein Cholesterol
HF: Heart Failure
HFpEF: Heart Failure with Preserved Ejection Fraction
HFrEF: Heart Failure with Reduced Ejection Fraction
HR: Hazard Ratio
LA: Left Atrium / Left Atrial
LAVI: Left Atrial Volume Index
LV: Left Ventricle / Left Ventricular
LVH: Left Ventricular Hypertrophy
LVMI: Left Ventricular Mass Index
LVVI: Left Ventricular Volume Index
MDCT: Multidetector Computed Tomography
MESA: Multi-Ethnic Study of Atherosclerosis
NT-proBNP: N-terminal Pro-Brain Natriuretic Peptide
PAF: Population Attributable Fraction
PAR: Population Attributable Risk
RCS: Restricted Cubic Spline
RR: Relative Risk
SBP: Systolic Blood Pressure
SD: Standard Deviation
SGLT2: Sodium-Glucose Cotransporter-2
STROBE: Strengthening the Reporting of Observational Studies in Epidemiology
T2DM: Type 2 Diabetes Mellitus
US: United States

Ethics approval and consent to participate

As a longitudinal population-based study sponsored by the National Institute of Health (NIH), MESA has received proper ethical oversight. The MESA protocol was approved by the Institutional Review Board (IRB) of the 6 field centers (Columbia University IRB, Johns Hopkins Medicine IRB, Northwestern University IRB, UCLA Office of the Human Research Protection Program (OHRPP), University of Minnesota Human Research Protection Program, Wake Forest Baptist Health IRB) and the National Heart, Lung, and Blood Institute. Data from participants who did not consent to commercial use were removed from our study.

Consent for publication

Not applicable.

Availability of data and materials

The datasets used and/or analyzed during the current study are available from the corresponding author on reasonable request.

Patient and public involvement

It was not appropriate or possible to involve patients or the public in the design, or conduct, or reporting, or dissemination plans of our research

Authors aggremnets

We confirm that the manuscript has been read and approved by all named authors and that there are no other persons who satisfied the criteria for authorship but are not listed. We further confirm that the order of authors listed in the manuscript has been approved by all of us.

We confirm that we have given due consideration to the protection of intellectual property associated with this work and that there are no impediments to publication, including the timing of publication, with

respect to intellectual property. In so doing we confirm that we have followed the regulations of our institutions concerning intellectual property.

We understand that the Corresponding Author is the sole contact for the Editorial process (including Editorial Manager and direct communications with the office). He is responsible for communicating with the other authors about progress, submissions of revisions and final approval of proofs. We confirm that we have provided a current, correct email address which is accessible by the Corresponding Author.

Funding

This research was supported by 2R42AR070713 and R01HL146666, R21OH012960 and MESA was supported by contracts 75N92020D00001, HHSN268201500003I, N01-HC-95159, 75N92020D00005, N01-HC- 95160, 75N92020D00002, N01-HC-95161, 75N92020D00003, N01- HC-95162, 75N92020D00006, N01-HC-95163, 75N92020D00004, N01-HC-95164, 75N92020D00007, N01-HC-95165, N01-HC-95166, N01-HC-95167, N01-HC-95168 and N01-HC-95169 from the National Heart, Lung, and Blood Institute, and by grants UL1-TR-000040, UL1-TR- 001079, and UL1-TR-001420 from the National Center for Advancing Translational Sciences (NCATS). Preparation of the manuscript was also supported by funding from HeartLung.AI. HeartLung Corporation is self-funded and NIH-SBIR funded. HeartLung SBIR funding number 1R43HL174376-01

CRediT authorship contribution statement

Seyed Reza Mirjalili: Writing – review & editing, Writing – original draft, Conceptualization. **Kyle Atlas:** Writing – review & editing, Writing – original draft, Formal analysis. **Anthony P. Reeves:** Writing – review & editing, Writing – original draft, Formal analysis. **Chenyu Zhang:** Writing – review & editing, Writing – original draft, Formal analysis. **Jakob Wasserthal:** Writing – review & editing, Writing – original draft. **Amir Azimi:** Writing – review & editing, Writing – original draft. **Ali Hashemi:** Writing – review & editing, Writing – original draft. **Mohammadhossein Mozafarybazargany:** Writing – review & editing, Writing – original draft. **Amir Ghaffari Jolfayi:** Writing – review & editing, Writing – original draft. **Thomas Atlas:** Writing – review & editing. **Claudia I. Henschke:** Writing – review & editing. **David F. Yankelevitz:** Writing – review & editing. **Javier J. Zulueta:** Writing – review & editing. **Jeffrey Mechanick:** Writing – review & editing. **Andrea D Branch:** Writing – review & editing. **Ning Ma:** Writing – review & editing. **Rowena Yip:** Writing – review & editing, Conceptualization. **Wenjun Fan:** Writing – review & editing. **Sion K. Roy:** Writing – review & editing. **Khurram Nasir:** Writing – review & editing. **Sabee Molloi:** Writing – review & editing. **Zahi Fayad:** Writing – review & editing. **Michael V. McConnell:** Writing – review & editing. **Ioannis A. Kakadiaris:** Writing – review & editing. **George Abela:** Writing – review & editing. **Rozemarijn Vliegenthart:** Writing – review & editing. **David J. Maron:** Writing – review & editing. **Jagat Narula:** Writing – review & editing. **Kim A. Williams Sr:** Writing – review & editing. **Prediman K. Shah:** Writing – review & editing. **Matthew J. Budoff:** Writing – review & editing. **Daniel Levy:** Writing – review & editing. **Roxana Mehran:** Writing – review & editing. **Robert A. Kloner:** Writing – review & editing. **Nathan D. Wong:** Writing – review & editing. **Morteza Naghavi:** Writing – review & editing, Writing – original draft, Conceptualization.

Declaration of competing interest

Several members of the writing group are inventors of the AI tool mentioned in this paper. M.N. is the founder of HeartLung.AI. A.P.R., T. A., D.F.Y., N.D.W., and D.L. are advisors to HeartLung.AI. C.Z. is a software engineer for HeartLung.AI. K.A. is a data scientist of HeartLung.AI. S.RM, A.A, A.H, M.M, A.G.J are research fellows for HeartLung.AI. M.V.M is Chief Health Officer for Toku, Inc. and advisor for Porter Health. D.J.M. reports research funding from Cleerly, Inc. and consultant fees from HeartFlow. The remaining authors declare no competing interests.

Acknowledgments

The authors thank the other investigators, the staff, and the participants of the MESA and Framingham Heart study for their valuable contributions.

Supplementary materials

Supplementary material associated with this article can be found, in the online version, at doi:10.1016/j.ajpc.2026.101656.

References

[1] Savarese G, Becher PM, Lund LH, Seferovic P, Rosano GMC, Coats AJS. Global burden of heart failure: a comprehensive and updated review of epidemiology. Cardiovasc Res 2022;118(17):3272–87.
[2] Wei C, Heidenreich PA, Sandhu AT. The economics of heart failure care. Prog Cardiovasc Dis 2024;82:90–101.
[3] McDonagh TA, Metra M, Adamo M, Gardner RS, Baumbach A, Böhm M, Burri H, Butler J, Čelutkienė J, Chioncel O. 2023 focused update of the 2021 ESC guidelines for the diagnosis and treatment of acute and chronic heart failure: developed by the task force for the diagnosis and treatment of acute and chronic heart failure of the European Society of Cardiology (ESC) with the special contribution of the Heart Failure Association (HFA) of the ESC. Eur Heart J 2023;44(37):3627–39.
[4] Chowdhary A, Jex N, Thirunavukarasu S, MacCannell A, Haywood N, Almutairi A, Athithan L, Jain M, Craven T, Das A, et al. Prospective Longitudinal Characterization of the Relationship between Diabetes and Cardiac Structural and Functional Changes. Cardiol Res Pract 2022;2022(1):6401180.
[5] Heidenreich PA, Bozkurt B, Aguilar D, Allen LA, Byun JJ, Colvin MM, Deswal A, Drazner MH, Dunlay SM, Evers LR, et al. 2022 AHA/ACC/HFSA guideline for the management of heart failure: a report of the American college of cardiology/American heart association joint committee on clinical practice guidelines. Circulation 2022;145(18):e895–1032.
[6] Sinha A, Gupta DK, Yancy CW, Shah SJ, Rasmussen-Torvik LJ, McNally EM, Greenland P, Lloyd-Jones DM, Khan SS. Risk-based approach for the prediction and prevention of heart failure. Circ Heart Fail 2021;14(2):e007761.
[7] Hippisley-Cox J, Coupland C. Diabetes treatments and risk of heart failure, cardiovascular disease, and all cause mortality: cohort study in primary care. BMJ 2016;354:i3477.
[8] Markman TM, Habibi M, Venkatesh BA, Zareian M, Wu C, Heckbert SR, Bluemke DA, Lima JAC. Association of left atrial structure and function and incident cardiovascular disease in patients with diabetes mellitus: results from multi-ethnic study of atherosclerosis (MESA). Eur Heart J - Cardiovasc Imaging 2017;18(10):1138–44.
[9] Miller RJH, Killekar A, Shanbhag A, Bednarski B, Michalowska AM, Ruddy TD, Einstein AJ, Newby DE, Lemley M, Pieszko K, et al. Predicting mortality from AI cardiac volumes mass and coronary calcium on chest computed tomography. Nat Commun 2024;15(1):2747.
[10] Berrington de González A, Mahesh M, Kim KP, Bhargavan M, Lewis R, Mettler F, Land C. Projected cancer risks from computed tomographic scans performed in the United States in 2007. Arch Intern Med 2009;169(22):2071–7.
[11] Naghavi M, Atlas K, Zhang C, Mao SS, Reeves AP, Budoff MJ, Henschke C, Yankelevitz D. AI-enabled cardiac chambers volumetry in non-contrast coronary artery calcium CT scans vs. contrast-enhanced coronary CT angiography scans in the same patients. Eur Heart J 2024;45(Supplement_1).
[12] Naghavi M, Reeves AP, Atlas K, Zhang C, Budoff MJ, Henschke C, Yankelevitz D. AI-enabled automated cardiac chambers volumetry in non-contrast ECG-gated cardiac scans vs. non-contrast non-gated lung scans. Eur Heart J 2024;45(Supplement_1).
[13] Naghavi M, Reeves A, Atlas K, Zhang C, Roy S, Budoff M, Henschke C, Yankelevitz D, Wong N, Levy D. Automated Left Ventricular Volumetry Using Artificial Intelligence In Coronary Calcium Scans (AI-CAC) Predicts Heart Failure Comparably To Cardiac MRI And Outperforms NT-proBNP: the Multi-ethnic Study Of Atherosclerosis (MESA). J Cardiovasc Comput Tomogr 2024;18(4):S16–7.
[14] Hijazi W, Shanbhag Aakash D, Miller Robert JH, Kavanagh P, Killekar A, Lemley M, Wopperer S, Knight S, Le Viet T, Mason S, et al. Deep learning derived anatomy from PET/CT attenuation maps and association with heart failure, myocardial infarction and death: multicenter study. JACC 2025;85(12_Supplement):1992.
[15] Naghavi M, Reeves Anthony P, Atlas Kyle C, Zhang C, Li D, Atlas T, Henschke Claudia I, Wong Nathan D, Roy Sion K, Budoff Matthew J, Yankelevitz David F. AI-enabled CT cardiac chamber volumetry predicts atrial fibrillation and stroke comparable to MRI. JACC: Adv 2024;3(11):101300.
[16] Naghavi M, Reeves A, Budoff M, Li D, Atlas K, Zhang C, Atlas T, Roy SK, Henschke CI, Wong ND, et al. AI-enabled cardiac chambers volumetry in coronary artery calcium scans (AI-CAC(TM)) predicts heart failure and outperforms NT-

proBNP: the multi-ethnic study of Atherosclerosis. J Cardiovasc Comput Tomogr 2024;18(4):392–400.
[17] Razipour A, Grodecki K, Manral N, Geers J, Gransar H, Shanbhag A, Miller RJH, Rozanski A, Berman DS, Slomka PJ, Dey D. AI-derived automated quantification of cardiac chambers and myocardium from non-contrast CT: prediction of major adverse cardiovascular events in asymptomatic subjects. Atherosclerosis 2025:401.
[18] Splansky GL, Corey D, Yang Q, Atwood LD, Cupples LA, Benjamin EJ, D'Agostino Sr RB, Fox CS, Larson MG, Murabito JM, et al. The third generation cohort of the national heart, lung, and blood institute's framingham heart study: design, recruitment, and initial examination. Am J Epidemiol 2007;165(11):1328–35.
[19] Feinleib M, Kannel WB, Garrison RJ, McNamara PM, Castelli WP. The Framingham offspring study. design and preliminary data. Prev Med 1975;4(4):518–25.
[20] Bild DE, Bluemke DA, Burke GL, Detrano R, Diez Roux AV, Folsom AR, Greenland P, Jacobs Jr DR, Kronmal R, Liu K, et al. Multi-ethnic study of atherosclerosis: objectives and design. Am J Epidemiol 2002;156(9):871–81.
[21] McKee PA, Castelli WP, McNamara PM, Kannel WB. The natural history of congestive heart failure: the Framingham study. N Engl J Med 1971;285(26):1441–6.
[22] Khan SS, Matsushita K, Sang Y, Ballew SH, Grams ME, Surapaneni A, Blaha MJ, Carson AP, Chang AR, Ciemins E, et al. Development and validation of the American heart association's prevent equations. Circulation 2024;149(6):430–49.
[23] Ernande L, Audureau E, Jellis CL, Bergerot C, Henegar C, Sawaki D, Czibik G, Volpi C, Canoui-Poitrine F, Thibault H, et al. Clinical implications of echocardiographic phenotypes of patients with diabetes mellitus. J Am Coll Cardiol 2017;70(14):1704–16.
[24] McDonagh TA, Metra M, Adamo M, Gardner RS, Baumbach A, Böhm M, Burri H, Butler J, Čelutkienė J, Chioncel O, et al. 2021 ESC guidelines for the diagnosis and treatment of acute and chronic heart failure: developed by the Task Force for the diagnosis and treatment of acute and chronic heart failure of the European Society of Cardiology (ESC) With the special contribution of the Heart Failure Association (HFA) of the ESC. Eur Heart J 2021;42(36):3599–726.
[25] 10. Cardiovascular disease and risk management: standards of care in diabetes-2026. Diabetes Care 2026;49(Supplement_1):S216–s245.
[26] Khan SS, Breathett K, Braun LT, Chow SL, Gupta DK, Lekavich C, Lloyd-Jones DM, Ndumele CE, Rodriguez CJ, Allen LA, et al. Risk-based primary prevention of heart failure: a scientific statement from the American heart association. Circulation 2025;151(20):e1006–26.
[27] Sharma K, Al Rifai M, Ahmed HM, Dardari Z, Silverman MG, Yeboah J, Nasir K, Sklo M, Yancy C, Russell SD, et al. Usefulness of coronary artery calcium to predict heart failure with preserved ejection fraction in men versus women (from the multi-ethnic study of atherosclerosis). Am J Cardiol 2017;120(10):1847–53.
[28] Bakhshi H, Ambale-Venkatesh B, Yang X, Ostovaneh MR, Wu CO, Budoff M, Bahrami H, Wong ND, Bluemke DA, Lima JAC. Progression of coronary artery calcium and incident heart failure: the multi-ethnic study of atherosclerosis. J Am Heart Assoc 2017;6(4).
[29] Kälsch H, Lehmann N, Möhlenkamp S, Neumann T, Slomiany U, Schmermund A, Stang A, Moebus S, Bauer M, Mann K, et al. Association of coronary artery calcium and congestive heart failure in the general population: results of the Heinz Nixdorf Recall study. Clin Res Cardiol 2010;99(3):175–82.
[30] de la Rosa AL, Mehta A, Hansen S, McClelland RL, Aldana-Bitar J, Kinninger A, Manubolu VS, Bertoni AG, Budoff MJ. Cardiac computed tomography imaging biomarkers for prediction of new-onset heart failure: multi-ethnic study of atherosclerosis. J Cardiovasc Comput Tomogr 2025;19(3):316–21.
[31] Leening MJ, Elias-Smale SE, Kavousi M, Felix JF, Deckers JW, Vliegenthart R, Oudkerk M, Hofman A, Steyerberg EW, Stricker BH, Witteman JC. Coronary calcification and the risk of heart failure in the elderly: the Rotterdam study. JACC Cardiovasc Imaging 2012;5(9):874–80.
[32] Huelsmann M. PONTIAC II: NT-proBNP selected prevention of cardiac events in diabetic patients. Medical University of Vienna; 2023.
[33] Huang G, Zhang L, Xie M, Fu M, Huang J, Lv Q. Assessment of left atrial function in diabetes mellitus by left atrial volume tracking method. J Huazhong Univ Sci Technolog Med Sci 2010;30(6):819–23.
[34] Muranaka A, Yuda S, Tsuchihashi K, Hashimoto A, Nakata T, Miura T, Tsuzuki M, Wakabayashi C, Watanabe N, Shimamoto K. Quantitative assessment of left ventricular and left atrial functions by strain rate imaging in diabetic patients with and without hypertension. Echocardiography 2009;26(3):262–71.
[35] Graça B, Ferreira MJ, Donato P, Gomes L, Castelo-Branco M, Caseiro-Alves F. Left atrial dysfunction in type 2 diabetes mellitus: insights from cardiac MRI. Eur Radiol 2014;24(11):2669–76.
[36] Gweon HM, Kim SJ, Kim TH, Lee SM, Hong YJ. Rim SJ: evaluation of left atrial volumes using multidetector computed tomography: comparison with echocardiography. Korean J Radiol 2010;11(3):286–94.
[37] To AC, Flamm SD, Marwick TH, Klein AL. Clinical utility of multimodality LA imaging: assessment of size, function, and structure. JACC Cardiovasc Imaging 2011;4(7):788–98.
[38] Hof IE, Velthuis BK, Van Driel VJ, Wittkampf FH, Hauer RN, Loh P. Left atrial volume and function assessment by magnetic resonance imaging. J Cardiovasc Electrophysiol 2010;21(11):1247–50.